MicroRNA-30c-2* limits expression of proadaptive factor XBP1 in the unfolded protein response

Andrew E. Byrd, Ileana V. Aragon, and Joseph W. Brewer

Department of Microbiology and Immunology, College of Medicine, University of South Alabama, Mobile, AL 36688

Stress in the endoplasmic reticulum (ER) triggers the unfolded protein response (UPR), a multifaceted signaling system coordinating translational control and gene transcription to promote cellular adaptation and survival. Microribonucleic acids (RNAs; miRNAs), single-stranded RNAs that typically function as posttranscriptional modulators of gene activity, have been shown to inhibit translation of certain secretory pathway proteins during the UPR. However, it remains unclear whether miRNAs regulate UPR signaling effectors directly. In this paper, we report that a star strand miRNA, miR-30c-2* (recently designated miR-30c-2-3p), is induced by the protein kinase RNA activated–like ER kinase (PERK) pathway of the UPR and governs expression of XBP1 (X-box binding protein 1), a key transcription factor that augments secretory capacity and promotes cell survival in the adaptive UPR. These data provide the first link between an miRNA and direct regulation of the ER stress response and reveal a novel molecular mechanism by which the PERK pathway, via miR-30c-2*, influences the scale of XBP1-mediated gene expression and cell fate in the UPR.

Introduction

Cells are highly sensitive to conditions that disrupt the environment of the ER or that increase demand on its machinery for synthesis, maturation, and transport of secretory cargo. Under such conditions of ER stress, cells launch the unfolded protein response (UPR) to balance client protein load with the folding capacity of the ER. Three distinct signaling pathways comprise the mammalian UPR and are initiated by the ER transmembrane sensor protein kinase RNA activated–like ER kinase (PERK), activating transcription factor 6 (ATF6), and inositol-requiring enzyme 1 (IRE1; Ron and Walter, 2007). Activated PERK phosphorylates the α subunit of eukaryotic initiation factor 2 (eIF2-α), effectively down-regulating protein synthesis (Harding et al., 2000b). Proteolytic processing of ATF6 yields an active transcription factor (Haze et al., 1999; Ye et al., 2000) that up-regulates expression of ER resident quality control proteins, including chaperones and ER-associated degradation (ERAD) components (Wu et al., 2007; Yamamoto et al., 2007; Adachi et al., 2008). Upon activation of IRE1, its endoribonuclease activity initiates an unconventional cytosolic splicing of *XBP1* mRNA, resulting in a translational frameshift that generates XBP1(S), a basic leucine zipper transcription factor (Shen et al., 2001; Yoshida et al., 2001; Calfon et al., 2002). XBP1(S) enhances a variety of ER and secretory pathway processes by up-regulating expression of genes involved in protein entry into the ER, protein folding and maturation, ERAD, and vesicular trafficking (Lee et al., 2003; Shaffer et al., 2004). If ER stress is not sufficiently alleviated by these adaptive mechanisms, the UPR can commit the damaged cell to death (Tabas and Ron, 2011).

XBP1 is subject to transcriptional, posttranscriptional, and posttranslational controls (Chen and Qi, 2010; Lee et al., 2011; Wang et al., 2011; Yanagitani et al., 2011; Majumder et al., 2012), indicating that the activity of this crucial UPR transcription factor is carefully balanced. MicroRNAs (miRNAs), ∼22-nt single-stranded RNAs that typically exert posttranscriptional control of gene activity (Bartel, 2009), represent a sizeable class of regulators, which outnumbers kinases and phosphatases (Leung and Sharp, 2010). A few ER stress-inducible miRNAs have been identified and shown to hinder translation of various secretory pathway proteins (Bartoszewski et al., 2011;

The Rockefeller University Press $30.00
J. Cell Biol. Vol. 196 No. 6   689–698
www.jcb.org/cgi/doi/10.1083/jcb.201201077

JCB   **689**

Behrman et al., 2011), suggesting that miRNAs play integral roles in the UPR. Therefore, we reasoned that miRNAs might participate in the exquisite regulation of XBP1. The obligate nature of miRNA biogenesis yields a pre-miRNA duplex. One strand of the duplex, the guide strand, is preferentially incorporated by an Argonaute protein into the RNA-induced silencing complex, promoting degradation or inhibiting translation of transcripts with base pair complementarity (Bartel, 2009). In contrast, the partner strand of the duplex, miRNA*, accumulates to lower levels than the guide strand and is generally assumed to be degraded (Ambros et al., 2003; Yang et al., 2011). However, emerging evidence indicates that miRNA* species can coaccumulate with their partner guide strand and mediate regulatory activity in various settings (Ro et al., 2007; Okamura et al., 2008; Yang et al., 2011). Here, we report discovery of a miRNA* that regulates expression of XBP1, thereby influencing XBP1-mediated gene expression and cell fate in the UPR.

Results and discussion

miR-30c-2* is a potential regulator of XBP1 expression

Using two computational algorithm programs, TargetScan (Lewis et al., 2005) and MicroCosm (Krek et al., 2005), we searched for miRNAs with potential base pair complementarities to conserved sequences in the *XBP1* mRNA 3′ untranslated region (UTR). This survey predicted a target site, featuring attributes of functional miRNA, for miR-30c-2* (recently designated miR-30c-2-3p) in the *XBP1* 3′ UTR (Fig. 1 A, left). First, the 7-nt sequence in the *XBP1* 3′ UTR exhibiting Watson–Crick pairing to positions 2–8, the "seed" region (Lewis et al., 2005), of miR-30c-2* is conserved across the three species assessed (Fig. 1 A, right). Second, miR-30c-2* includes a conserved 5′ U (Fig. 1 A, left). Sequence analysis of miRNA* strand populations has revealed a strong disfavor for 5′ G, a feature avoided by recognized miRNA regulatory strands (Frank et al., 2010; Yang et al., 2011). Finally, the sequences of both miR-30c-2* and its guide strand, miR-30c (recently designated miR-30c-2-5p; Fig. 1 B), are identical across numerous species, including *Homo sapiens* and *Mus musculus* (Fig. 1 C). Cross-species conservations of the miRNA sequence, the seed region, and a 5′ U are all key characteristics of endogenous functional miRNA (Lai, 2002; Krek et al., 2005; Lewis et al., 2005). Notably, our bioinformatics analysis did not reveal a target site in the *XBP1* 3′ UTR for the corresponding guide strand miR-30c.

To test the capacity of miR-30c-2* to exert regulatory activity via its putative target site in the *XBP1* 3′ UTR, we constructed reporter vectors containing a single copy of either the wild-type target sequence or an altered seed region (mutant [MUT]; Fig. 2 A) positioned 3′ of a *firefly luciferase* gene. Overexpression of miR-30c-2* in NIH-3T3 fibroblasts reduced the activity of the luciferase reporter containing the wild-type target sequence but not of the luciferase reporter containing the MUT target site (Fig. 2 A). Therefore, miR-30c-2* is functionally competent and recognizes the predicted cognate *XBP1* 3′ UTR target site in a sequence-specific manner. Next, we asked whether miR-30c-2* can alter the expression

of endogenous *XBP1*. Overexpression of miR-30c-2* in HeLa cells attenuated induction of both *XBP1* mRNA (Fig. 2 B) and XBP1(S) protein (Fig. 2 C) in response to tunicamycin (Tm), an inhibitor of N-linked glycosylation that triggers the UPR. In agreement with these data, the induction of XBP1-dependent, ER stress-responsive genes (Lee et al., 2003; Adachi et al., 2008) *SEC23B* (Fig. 2 D), which encodes a cargo receptor involved in vesicle trafficking, and *DNAJB9* (Fig. S1 A), which encodes the ER chaperone cofactor ERdj4, in response to Tm was severely impaired in cells overexpressing miR-30c-2*. In contrast, we observed normal induction of the XBP1-independent UPR target gene *DDIT3* (encodes CCAAT enhancer-binding protein homologous protein [CHOP]; Fig. S1 B; Lee et al., 2003), indicating the presence of an intact UPR in this system. These data establish that miR-30c-2* has the capacity to limit induction of *XBP1* mRNA, XBP1(S) protein, and XBP1-dependent target genes. XBP1(S) positively regulates *XBP1* gene transcription (Yoshida et al., 2001); hence, miR-30c-2* could regulate *XBP1* expression by impeding translation of XBP1(S) and/or promoting degradation of *XBP1* transcripts (Huntzinger and Izaurralde, 2011).

ER stress-mediated induction of miR-30c-2* involves the PERK pathway and nuclear factor κB (NF-κB)

As a potential regulator of *XBP1*, we reasoned that expression of miR-30c-2* might be modulated during the UPR. We found that treatment of cells with either Tm or thapsigargin (Tg), an inhibitor of the ER Ca^{2+} ATPase and a strong inducer of the UPR, up-regulates expression of miR-30c-2* (Fig. 3 A). Using gene knockout mouse embryo fibroblasts (MEFs) and their wild-type counterparts, we then determined that ER stress-induced expression of miR-30c-2* is dependent on the PERK pathway of the UPR, whereas ATF6-α and IRE1-α are dispensable for this event (Fig. 3 B).

PERK-mediated down-regulation of global protein synthesis leads, paradoxically, to increased translation of ATF4 (Harding et al., 2000a), a factor that drives expression of a variety of targets, including the proapoptotic transcription factor CHOP, enzymes that reduce oxidative stress, and proteins that function in amino acid metabolism (Harding et al., 2003). In addition, the PERK pathway activates NF-κB, a dimer of Rel family proteins that regulates a myriad of genes involved in inflammation, stress responses, cell growth, and apoptosis (Karin et al., 2002; Li and Verma, 2002). In its inactive state, NF-κB is sequestered in the cytoplasm bound to proteins known as inhibitors of NF-κB (IκB; Baeuerle and Baltimore, 1988). PERK-mediated repression of protein synthesis depletes the cytosolic pool of IκB, freeing NF-κB to enter the nucleus and activate target genes (Jiang et al., 2003; Deng et al., 2004). Bioinformatics analysis revealed a potential NF-κB binding site (5′-GGGGG-CTTTAT-3′) ∼1.8 kb upstream of the mapped miR-30c-2* chromosomal location. This candidate NF-κB binding site, exhibiting a 2-nt mismatch with the NF-κB consensus sequence (5′-gggRNNYYCC-3′; the lowercase letters indicate the most common nucleotide in a variable position), was previously implicated as a functional NF-κB enhancer element in the tumor
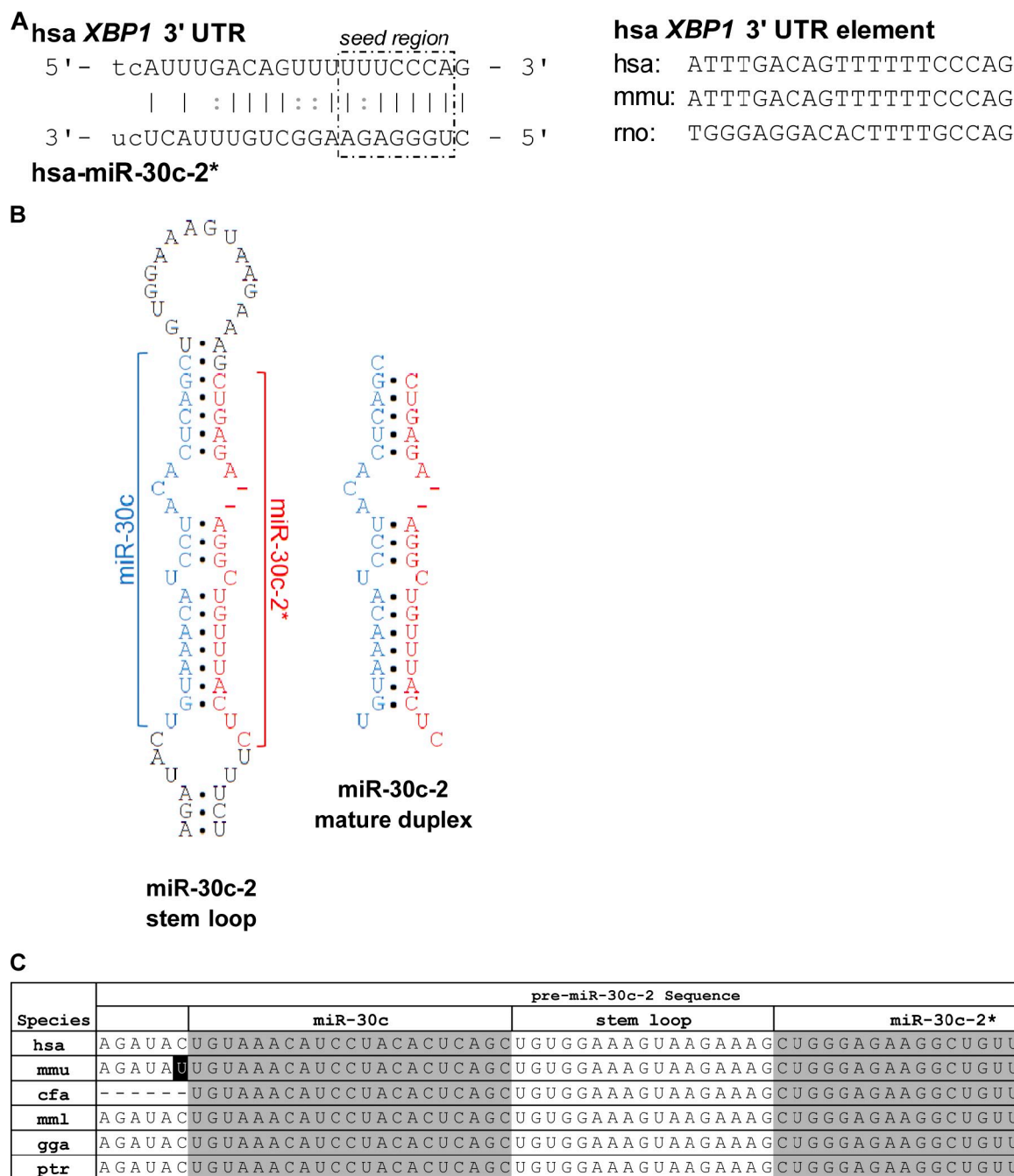
A **hsa *XBP1* 3' UTR**

seed region

```
5'- tcAUUUGACAGUUUUUUCCCAG - 3'
      |  |  :|||||::||:|||||||
3'- ucUCAUUUGUCGGAAGAGGGUC - 5'
```

hsa-miR-30c-2*

hsa *XBP1* 3' UTR element

hsa: ATTTGACAGTTTTTTCCCAG
mmu: ATTTGACAGTTTTTTCCCAG
rno: TGGGAGGACACTTTTGCCAG

B

miR-30c-2
stem loop

miR-30c-2
mature duplex

C

Figure 1. **miR-30c-2* is a potential regulator of XBP1 expression.** (A, left) Sequence alignment of the predicted duplex formation between miR-30c-2* and nucleotides 605–625 within the human *XBP1* 3′ UTR. (right) Cross-species homology of the predicted miR-30c-2* binding site within the human (*H. sapiens* [*hsa*]), mouse (*M. musculus* [*mmu*]), and rat (*Rattus norvegicus* [*rno*]) *XBP1* 3′ UTR. Lines indicate complementarity; dots indicate GU wobble. (B) Stem loop structure and mature duplex of human miR-30c-2. (C) Sequence alignment of the miR-30c-2 stem loop for several species (miRBase sequence database), including *H. sapiens, M. musculus, Canis familiaris* (*cfa*), *Macaca mulatta* (*mml*), *Gallus gallus* (*gga*), and *Pan troglodytes* (*ptr*). Black highlighted letters show a nucleotide that differs from the nucleotide in the corresponding position in the *hsa* sequence. Dashes show nucleotide sequences not provided in miRBase database.

necrosis factor α promoter (Shakhov et al., 1990). Additional searches for transcription factor binding sites upstream of miR-30c-2* revealed no known or predicted binding sites for either ATF4 or CHOP. Therefore, we tested whether ER stress–induced expression of miR-30c-2* involves NF-κB. Overexpression of a constitutively active, dominant-negative IκB-α MUT (Brockman et al., 1995) attenuated induction of miR-30c-2* in response to Tm (Fig. 3 C). We then used chromatin immunoprecipitation (ChIP) to determine whether NF-κB binds to the predicted motif upstream of miR-30c-2* during the UPR. The analysis revealed a greater than eightfold enrichment of NF-κB at this region after 6 h of Tm treatment (Fig. 3 D). These data (Fig. 3, B–D) suggest that NF-κB, downstream of PERK, plays a critical role in up-regulating expression of miR-30c-2* in the Tm-induced UPR.
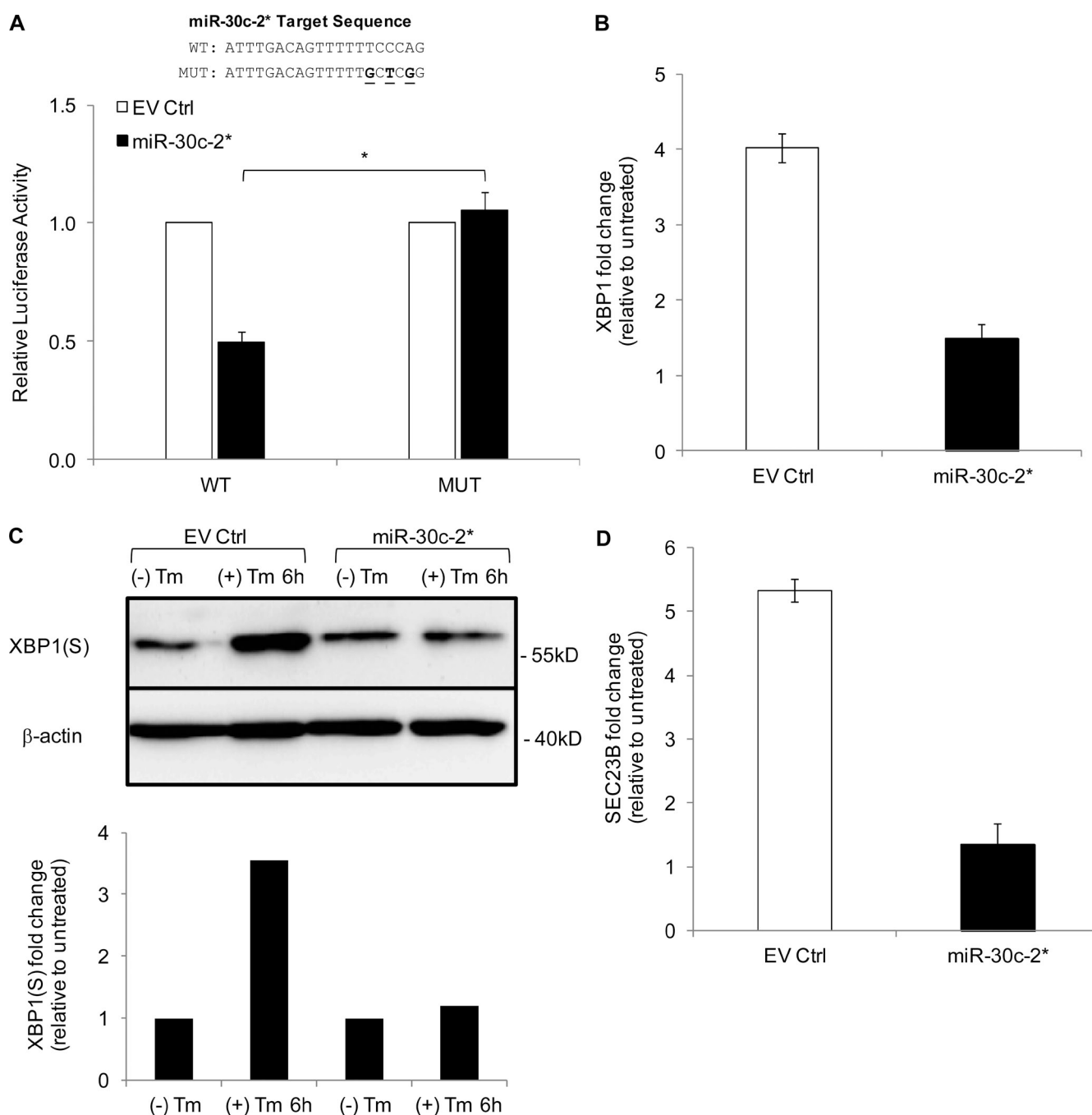
Figure 2. **miR-30c-2* is competent to target a predicted recognition site within the 3′ UTR of *XBP1* mRNA and negatively regulate *XBP1* expression.** (A) Firefly luciferase activity of the wild-type (WT) and mutant (MUT; mutations underlined) *XBP1* 3′ UTR reporter gene in NIH-3T3 cells transfected with either a miR-30c-2*–GFP expression vector (miR-30c-2*) or an empty GFP vector (empty vector control [EV Ctrl]). Data are plotted as firefly luciferase activity relative to that observed in empty vector control cells (set at 1; *, P < 0.05). (B–D) HeLa cells were transfected with either an miR-30c-2*–GFP expression vector (miR-30c-2*) or an empty GFP vector and either left untreated or treated with Tm for 6 h. (B and D) Real-time qRT-PCR analysis of *XBP1* (B) and *SEC23B* (D) expression in GFP⁺ cells isolated by FACS; data are plotted as fold change in mRNA in treated versus untreated cells (set at 1). (C) Immunoblot analysis of XBP1(S) and β-actin (top) and the corresponding quantitative data plotted as fold change in XBP1(S) protein, normalized to β-actin, in treated versus untreated cells (set at 1; bottom) are from a single representative experiment out of three repeats. Data are means ± SD.

miR-30c-2* regulates XBP1 expression and the magnitude of XBP1-mediated gene transcription

We next sought to determine whether endogenous miR-30c-2* indeed targets *XBP1* mRNA. We treated HeLa cells with Tm for 2–18 h and assessed the kinetics of induction for both miR-30c-2* and *XBP1*. As expected, *XBP1* was induced early (2 h) and peaked at ∼6 h of Tm treatment (Fig. 4 A). Interestingly, miR-30c-2* was moderately induced as early as 2 h of Tm treatment and was maximal around 6 h (Fig. 4 A). A similar expression profile was observed in Tm-treated NIH-3T3 cells (Fig. S2). The concomitant up-regulation of miR-30c-2* and *XBP1* mRNA suggested that miR-30c-2* might influence *XBP1* expression as the UPR proceeds. If so, we reasoned that inhibiting miR-30c-2*
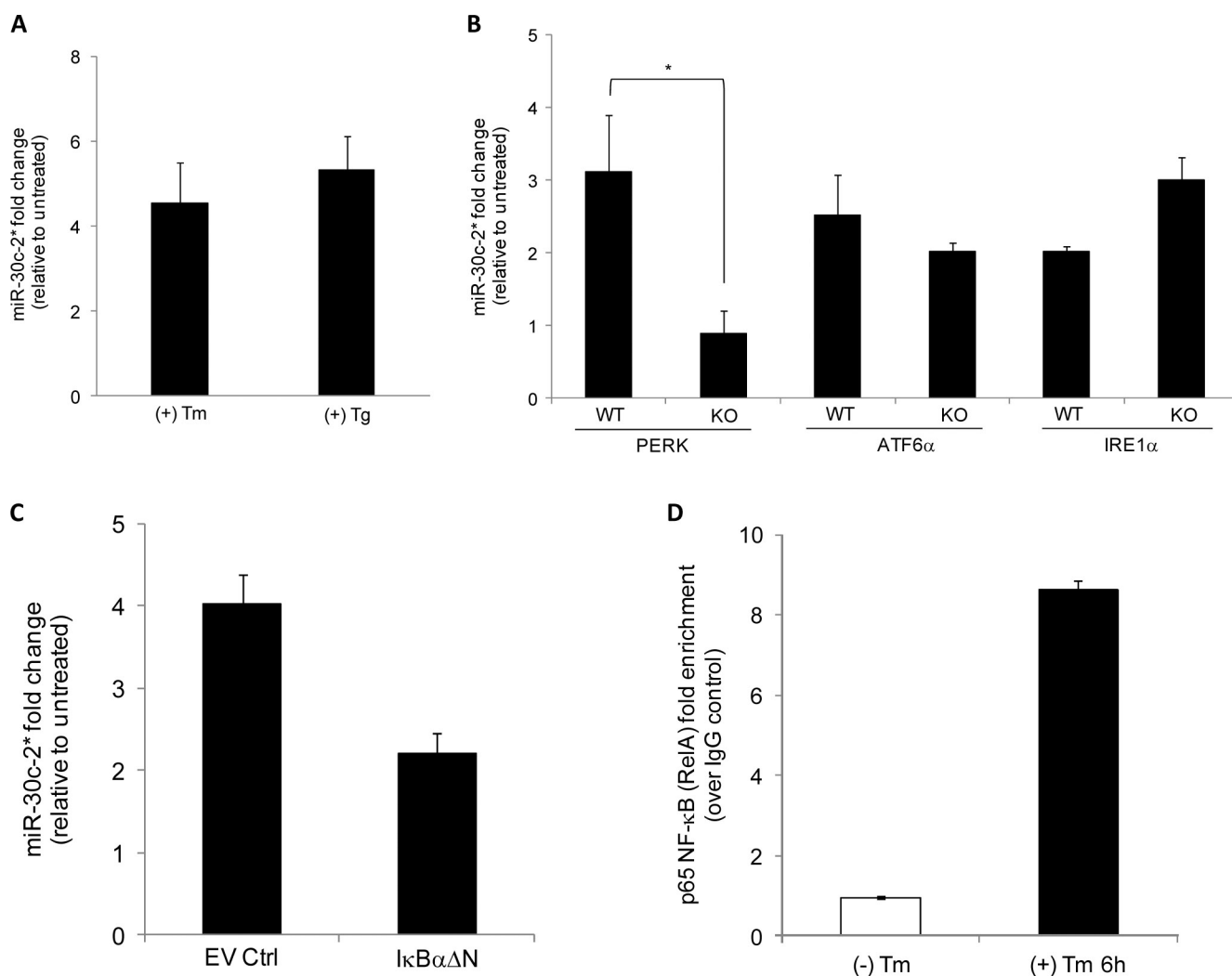
Figure 3. **ER stress-mediated induction of miR-30c-2* involves the PERK pathway and NF-κB.** (A–C) qRT-PCR analysis of miR-30c-2*; data are plotted as fold change in miR-30c-2* in treated versus untreated cells (set at 1; *, P < 0.05). (A) NIH-3T3 cells untreated or treated with Tm or Tg for 6 h. (B) PERK$^{-/-}$, ATF6-α$^{-/-}$, IRE1-α$^{-/-}$ (knockout [KO]) and corresponding wild-type (WT) MEFs untreated or treated with Tm for 6 h. (C) NIH-3T3 cells transfected with either an IκB-α dominant-negative expression vector (IκBαΔN) or the corresponding empty vector control (EV Ctrl) and either left untreated or treated with Tm for 6 h. (D) ChIP analysis of NF-κB p65(RelA) at a putative NF-κB binding site ~1.8 kb upstream of the mapped miR-30c-2* chromosomal location in untreated and Tm-treated (6 h) NIH-3T3 cells. Data are plotted as the fold enrichment of the appropriate PCR product obtained by immunoprecipitation with an anti-p65(RelA) antibody versus a control IgG. Data are means ± SD.

accumulation during the UPR would result in increased levels of *XBP1* mRNA and XBP1(S) protein. To test this hypothesis, we stably expressed an miRNA inhibitor specific for miR-30c-2* in HeLa cells. In cells expressing anti–miR-30c-2*, the accumulation of miR-30c-2* in response to Tm was ablated at peak induction times (4 and 6 h; Fig. 4 B). Conversely, when treated with Tm, cells expressing anti–miR-30c-2* exhibited greater induction of *XBP1* mRNA (Fig. 4 C), XBP1(S) protein (Fig. 4 D) and XBP1-dependent, ER stress-responsive genes (Lee et al., 2003; Adachi et al., 2008) *SEC23B* (Fig. 4 E), *DNAJB9*, *SRP54A*, which encodes a subunit of the signal recognition particle, and *EDEM1*, which encodes an ERAD component (Fig. S3, A–C). Again, we observed normal induction of the XBP1-independent UPR target gene *DDIT3* (Fig. S3 D). These findings demonstrate that endogenous miR-30c-2* regulates expression of *XBP1* during the UPR and, in turn, modulates the magnitude of XBP1(S)-mediated gene transcription.

miR-30c-2* influences cell fate under conditions of ER stress

Expression of XBP1(S) and its downstream target genes is considered to be proadaptive in the UPR. Therefore, to further investigate the impact of endogenous miR-30c-2* on the overall cellular response to ER stress, we assessed the fate of HeLa cells expressing either the anti–miR-30c-2* or the inhibitor control after an extended period of UPR activation. At 0, 24, and 30 h of Tm treatment, cells were stained with 7-aminoactinomycin D (7-AAD), a fluorescent DNA intercalator dye that penetrates the compromised membranes of late-stage apoptotic or necrotic cells, and analyzed by flow cytometry. Indeed, the percentage of cells scoring as 7-AAD permeable was attenuated by anti–miR-30c-2* at all intervals tested (Fig. 5, A and B, 7-AAD Pos). To determine whether this anti–miR-30c-2* effect was in fact XBP1 dependent, we performed similar experiments in wild-type and XBP1-deficient MEFs.
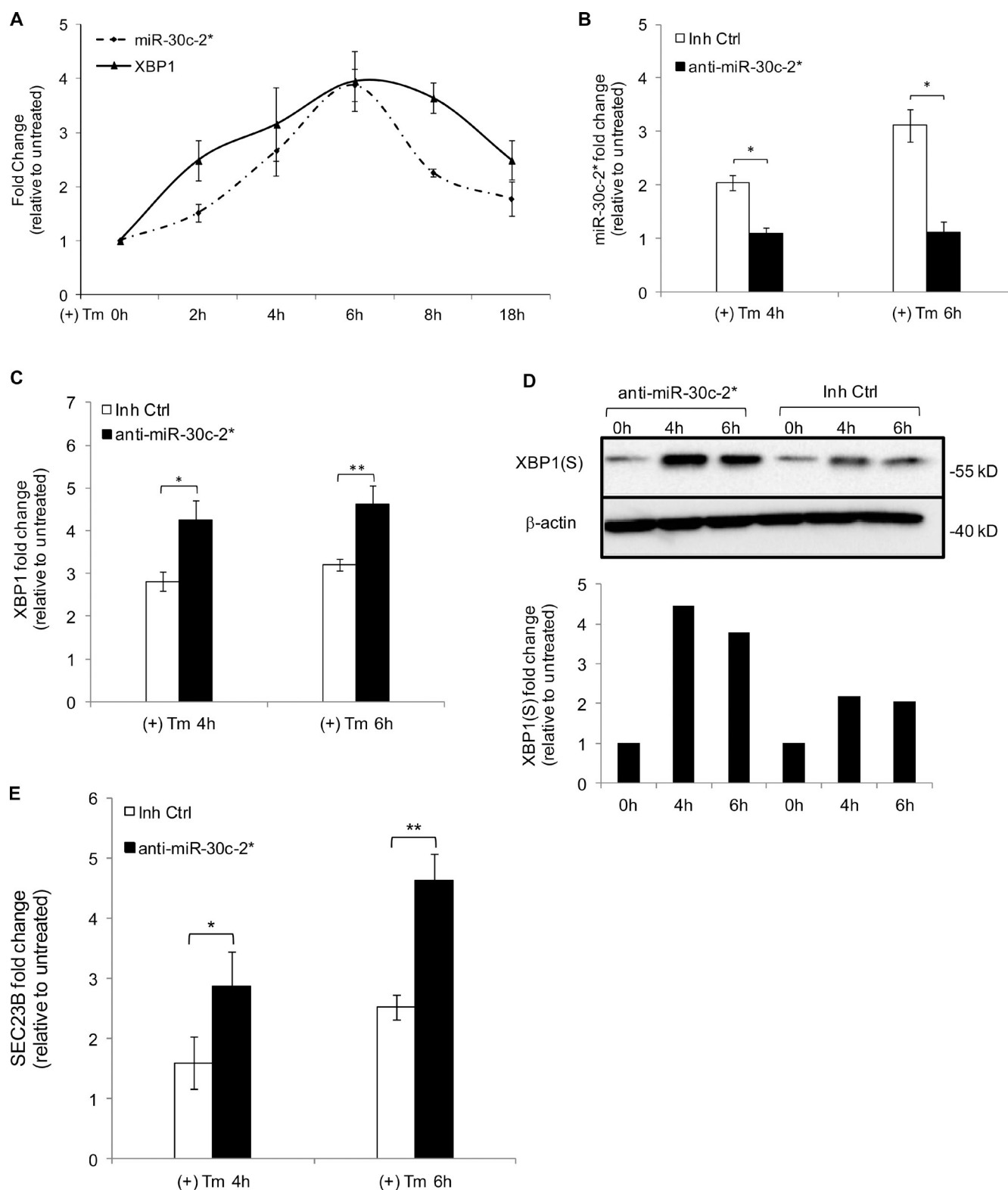
Figure 4. **Endogenous miR-30c-2* negatively regulates *XBP1* expression in the UPR.** (A) qRT-PCR analysis of miR-30c-2* and *XBP1* mRNA in HeLa cells treated with Tm for the indicated intervals; data are plotted as fold change in treated versus untreated cells (set at 1). (B–E) Analysis of HeLa cells stably expressing either a miR-30c-2*–specific inhibitor (anti–miR-30c-2*) or a control scrambled inhibitor (Inh Ctrl) and either left untreated or treated with Tm for the indicated intervals. (B, C, and E) qRT-PCR analysis of miR-30c-2* (B), *XBP1* mRNA (C), and *SEC23B* mRNA (E); data are plotted as fold change in treated versus untreated cells (set at 1). (D) Immunoblot analysis of XBP1(S) and β-actin (top) and the corresponding quantitative data plotted as fold change in XBP1(S) protein, normalized to β-actin, in treated versus untreated cells (set at 1; bottom) are from a single representative experiment out of three repeats. Data are means ± SD. *, P < 0.05; **, P < 0.03.
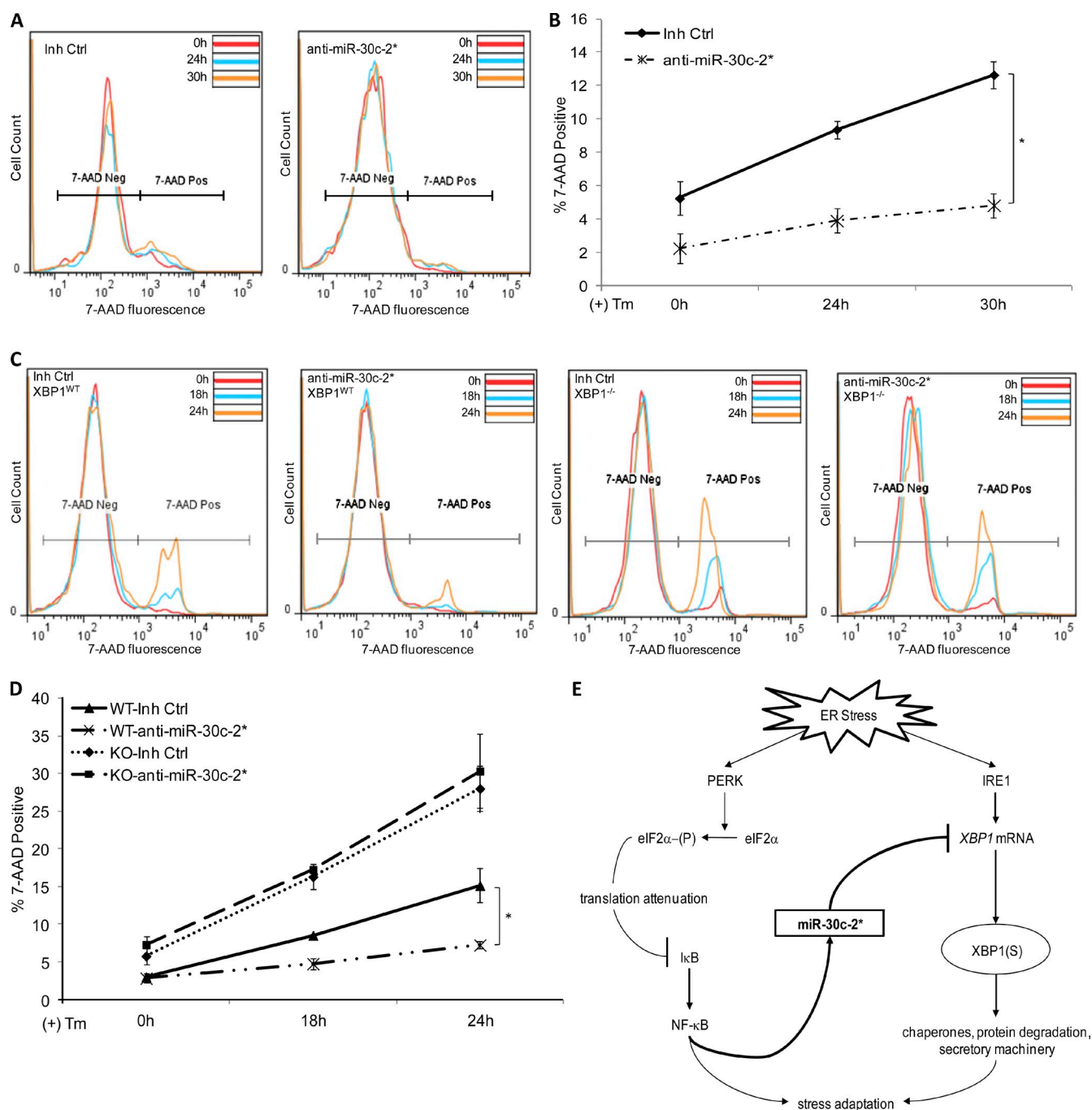
Figure 5. **miR-30c-2* influences the fate of cells challenged with ER stress.** (A and B) HeLa cells stably expressing either an miR-30c-2*–specific inhibitor (anti–miR-30c-2*) or a control scrambled inhibitor (Inh Ctrl) were left untreated or treated with Tm for the indicated intervals, stained with 7-AAD, and analyzed by flow cytometry. (A) Histograms discriminating viable (7-AAD negative [Neg]) from dead (7-AAD positive [Pos]) cells. (B) Quantitative analysis of 7-AAD–positive cells during Tm-induced ER stress. Note that anti–miR-30c-2* provided measurable improvement in the viability of untreated cells (0 h), consistent with basal UPR signaling and XBP1(S) expression under these conditions (Fig. 4 D, top). (C and D) XBP1^{WT} (wild-type [WT]) and XBP1$^{-/-}$ (knockout [KO]) MEFs transiently expressing either anti–miR-30c-2* or a control scrambled inhibitor were left untreated or treated with Tm for the indicated intervals and analyzed as in A. (C) Histograms discriminating viable (7-AAD negative) from dead (7-AAD positive) cells. (D) Quantitative analysis of 7-AAD–positive cells during Tm-induced ER stress. (E) Model for miR-30c-2* as a regulatory interface between the PERK and IRE1–XBP1 pathways in the UPR, regulating XBP1 expression, the strength of XBP1-mediated gene transcription, and cellular adaptation to ER stress. Data are means ± SD. *, P < 0.05. P, phospho.

As expected, XBP1-deficient MEFs exhibited heightened sensitivity to Tm-induced toxicity as compared with wild-type MEFs (Fig. 5 C). Importantly, expression of anti–miR-30c-2* protected wild-type, but not XBP1-deficient, MEFs against Tm-induced death (Fig. 5, C and D).

Recent studies have unveiled ER stress-inducible miRNAs that negatively regulate translation of certain secretory pathway proteins (Bartoszewski et al., 2011; Behrman et al., 2011), affording cells another means of balancing protein load with ER capacity. In contrast, our finding that ER stress-inducible miR-30c-2*

regulates expression of *XBP1* is the first discovery of a miRNA that directly modulates a UPR effector. Moreover, our data reveal a novel regulatory interface between the PERK and IRE1–XBP1 pathways that involves NF-κB and miR-30c-2* (Fig. 5 E). It seems counterintuitive that miR-30c-2* exists to compromise cellular stress tolerance by extinguishing XBP1. Rather, we reason that overzealous expression of XBP1(S) might be deleterious depending on the nature, intensity, and duration of physiological conditions that increase demands on the ER. By buffering the level of XBP1(S), miR-30c-2* could contribute to the delicate balance between pro- and maladaptive outcomes in the UPR. Interestingly, a recent study revealed that *XBP1(S)* mRNA is stabilized early in the UPR and then becomes increasingly labile (Majumder et al., 2012). In light of our data, it is intriguing to speculate that the accumulation of miR-30c-2* accelerates the turnover of *XBP1(S)* mRNA as the UPR progresses.

In addition to its link to the PERK pathway, NF-κB can be activated downstream of many signaling molecules, including IRE1 (Kaneko et al., 2003; Hu et al., 2006), Toll-like receptors (Kawai and Akira, 2010), and cytokine receptors (Li and Verma, 2002). This raises the interesting possibility that certain stimuli not obviously associated with ER stress, such as cytokines that induce NF-κB, might influence XBP1 via miR-30c-2*. We hypothesize that the relative contribution of miR-30c-2* to the "fine tuning" of XBP1 activity may vary in distinct tissue-, developmental-, and stress-specific settings in which the entire UPR or individual UPR pathways are engaged. It will be particularly interesting to investigate the degree to which miR-30c-2* influences gene expression, cell function, and cell fate in normal as well as pathophysiologic processes that involve XBP1, such as plasma cell differentiation (Iwakoshi et al., 2003), macrophage activation by Toll-like receptor signaling (Martinon et al., 2010), and tumor cell survival (Romero-Ramirez et al., 2004). Finally, our data add miR-30c-2* to a small but growing list of mammalian miRNA* species with defined regulatory activities (Yang et al., 2011), underscoring that miRNA* strands play critical roles in gene regulation.

Materials and methods

Cell culture and transfections
NIH-3T3 fibroblasts, MEFs, and HeLa cells were cultured as previously described (Bommiasamy et al., 2009). IRE1-α$^{-/-}$, XBP1$^{-/-}$, and ATF6-α$^{-/-}$ and corresponding wild-type MEF cell lines were provided by R.J. Kaufman (University of Michigan, Ann Arbor, MI). PERK$^{-/-}$ and corresponding wild-type MEF cell lines were provided by D. Ron (University of Cambridge, Cambridge, England, UK). Cells were transfected using either a calcium phosphate method or Lipofectamine 2000 (Invitrogen). For transient transfection, NIH-3T3 cells were seeded at either 7×10^4 cells/60-mm dish or 3×10^4 cells/well on 6-well plates, HeLa cells were seeded at either 10^6 cells/60-mm dish or 5×10^5 cells/well on 6-well plates, and MEFs were seeded at 10^5 cells/60-mm dish. To generate cell lines stably expressing anti-miRNAs, HeLa cells were seeded at 3×10^6 cells/100-mm dish, transfected with Lipofectamine 2000, and then selected in 3 µg/ml puromycin (MediaTech) for 7 d after transfection. Death of all nontransfected control cells was achieved by day 5 after transfection. To induce ER stress, cells were treated with either 1 µg/ml Tm (Sigma-Aldrich) or 0.4 µM Tg (EMD) for various intervals.

Bioinformatic sequence analysis
miRNA sequences were retrieved from the miRBase sequence database. Prediction of miRNA target sites in the *XBP1* 3′ UTR was conducted using two algorithm-based software programs, TargetScan (Whitehead Institute for Biomedical Research) and MicroCosm (European Bioinformatics Institute). Potential transcription factor binding sites upstream of the miR-30c-2* chromosomal location were identified using the NSITE program (Softberry) and the University of California, Santa Cruz Genome browser.

Reporter and expression vectors
The pMIR-XBP1$^{WT605–625}$ and pMIR-XBP1^{Mut} luciferase reporter vectors were constructed using oligonucleotides (40 base pairs) containing a single copy of either the wild-type or MUT putative miR-30c-2* target sequence present in the human *XBP1* 3′ UTR (Integrated DNA Technologies). The MUT fragment includes target-abolishing substitutions in nucleotides 1 (A to G), 3 (C to T), and 5 (T to G) of the miR-30c-2* seed region. Both the wild-type and MUT fragment contained a BlpI site used in screening transformants. Fragments were ligated into the SpeI–HindIII sites of the pMIR-REPORT vector (Applied Biosystems), with *firefly luciferase* as the primary reporter gene. The pCMV–Renilla luciferase vector (Promega) provides constitutive expression of Renilla luciferase. The pCMV-miR-30c-2 and pCMV-miR-empty vector (OriGene) contain a cassette encoding GFP. pCMV-miR-30c-2 provides constitutive expression of both miR-30c and miR-30c-2*. The miArrest vectors (GeneCopoeia) pEZX-AM02-anti–miR-30c-2* and pEZX-AM02 inhibitor control contain cassettes encoding puromycin resistance and mCherry. The pEZX-AM02-anti–miR-30c-2* vector provides constitutive expression of an miR-30c-2*–specific inhibitor, and the pEZX-AM02 inhibitor control yields a scrambled, nonspecific anti-miRNA. The posttranscriptional processing of the anti-miRNA expressed from miArrest miRNA inhibitor vectors yields a structure that hybridizes with two molecules of the target miRNA, thereby trapping the miRNA and preventing it from exerting regulatory activity. The pCDNA3.1-IκB-αΔN vector, provided by W. Lin (University of South Alabama, Mobile, AL), encodes a truncated IκB-α lacking the amino-terminal 36 amino acids required for signal-induced degradation (Brockman et al., 1995).

RNA isolation and quantitative real-time RT-PCR
RNAs were extracted from cells using either the miRNeasy Mini Kit for miRNA analysis or the RNeasy Plus Mini Kit (QIAGEN), and 300 ng total RNA was reverse transcribed using an RT-PCR system (miRcury LNA Universal RT microRNA PCR; Exiqon) for miRNA analysis and the reverse transcription system (ImProm-II; Promega) for mRNA analysis. Resulting cDNA from miRNA and mRNA were diluted 1:80 and 1:40, respectively. Real-time PCR was performed using a thermocycler (C1000; Bio-Rad Laboratories) with an optic module real-time detection system (CFX96; Bio-Rad Laboratories). Reactions were performed in triplicate using the SYBR green supermix (IQ; Bio-Rad Laboratories). miR-30c-2* was amplified using primers (LNA; Exiqon). Forward and reverse primers used are as follows: 5′-TAGAAAGAAAGCCCGGATGAGCGA-3′ and 5′-GTGTC-CATTCCCAAGCGTGTTCTT-3′ (mouse *XBP1*); 5′–AAGGCTCGAATGAGT-GAGCTGGAA-3′ and 5′-TCCTGGTTCTCAACTACAAGGCCA-3′ (human *XBP1*); 5′-AGTCATTGCCTTTCTCCTTCGGGA-3′ and 5′-AAGCAGGGTCA-AGAGTGGTGAAGA-3′ (human *DDIT3*); 5′-AGCAGCAGCATTCTAGCT-GACAGA-3′ and 5′-GCCTGCAGAAGGTGCTTGAAGTTT-3′ (human *SEC23B*); 5′-CCCGCCTCACATTGAAATCC-3′ and 5′-GCGTATGTATCA-GTCTCAGTGG-3′ (mouse *β2M*); 5′-AGATGAGTATGCCTGCCGTGT-GAA-3′ and 5′-TGCTGCTTACATGTCTCGATCCCA-3′ (human *β2M*); 5′-AAGGGAGTGTGTGCGAGTTGTCTA-3′ and 5′-AATTCGTCGAGA-TCGTGCACCCTT-3′ (human *DNAJB9*); 5′-TGGACACCGACTAAGG-GAAAGCAA-3′ and 5′-TGGTCAAACGCTCCTGCTCTGAAT-3′ (human *SRP54A*); and 5′-TCTTAGCTCTGCAGCCACCGTAAA-3′ and 5′-TGGA-ACCTCCATACACTGGTCCAT-3′ (human *EDEM1*). miRNA and transcript levels were normalized to β2-microglobulin mRNA levels (ΔCT), and the normalized data were used to determine changes in gene expression ($2^{-\Delta\Delta CT}$). To analyze the effect of Tm treatment on target gene expression, untreated samples were set as a calibrator (control) and compared with their respective treated samples.

Luciferase reporter assays
NIH-3T3 cells were transfected with pCMV–Renilla luciferase plus either pMIR-XBP1$^{WT605–625}$, pMIR-XBP1^{Mut}, or pMIR-REPORT in combination with either pCMV-miR-30c-2 or pCMV–empty vector. At 24 h after transfection, cell lysates were prepared and assayed for both Renilla and firefly luciferase activity using a reporter assay kit (Dual-Luciferase Reporter Assay; Promega). Firefly luciferase activity was normalized to Renilla luciferase activity. Assays were performed in triplicate for a minimum of three independent experiments.

Preparation of cell extracts and immunoblotting

Cell lysates were prepared using lysis buffer (0.25 M Tris-HCl/0.2% SDS, pH 6.8, 20% glycerol, 4% SDS, 10 mM β-glycerol phosphate, and 1 µl/ml protease inhibitor cocktail [Sigma-Aldrich]). Clarified lysates were assayed for protein content using a protein assay (DC; Bio-Rad Laboratories) and bovine serum albumin as standards. Equivalent amounts of protein were added to an equal volume of 2× sample buffer (125 mM Tris-HCl, pH 6.8, 10% 2-mercaptoethanol, 20% glycerol, 4% SDS, and 0.02% bromophenol blue) and separated by electrophoresis in 10% SDS-polyacrylamide gels. Proteins were electrophoretically transferred to membranes (Immobilon-P; Millipore) using a 3-cyclohexylamino-1-propanesulfonic acid–buffered system and placed in blocking buffer (PBS, pH 7.4, 5% nonfat milk, and 0.1% Tween 20 [PBS-T]). Immunoblotting was performed using a mouse anti–human XBP1(S) antibody (catalog no. 647502; BioLegend), a mouse anti–β-actin antibody (Sigma-Aldrich), a rabbit horseradish peroxidase–conjugated anti–mouse IgG antibody (Cell Signaling Technology), and enhanced chemiluminescence substrate (Super Signal West Dura; Thermo Fisher Scientific) chemiluminescence reagents. Signals were captured using an imaging system (LAS-1000; Fujifilm) and quantified using Image Gauge v4.0 software (Fujifilm).

ChIP assay

Chromatin was prepared using the enzymatic ChIP kit (ChIP-IT Express; Active Motif) as described in the manufacturer's protocol and subjected to immunoprecipitation using an anti–NF-κB p65(RelA) antibody (catalog no. 17-10060; Millipore) and an IgG control antibody. The recovered DNA was subjected to PCR using a forward primer, 5′-ATACAGAGCCTTAC-CAACTGCCAC-3′, and reverse primer, 5′-AAGCATCACCAAAGCT-TCCTGG-3′, to amplify a 131–base pair segment including the putative NF-κB p65(RelA) binding site. Fold enrichment was determined by first solving for the DNA quantity of the NF-κB p65(RelA) ChIP and IgG samples and then calculating the fold enrichment of the NF-κB p65(RelA) ChIP relative to the IgG sample. As controls, successful immunoprecipitation of NF-κB p65(RelA)-associated DNA fragments was verified by quantitative RT-PCR (qRT-PCR) using ChIP primers specific for the IκB-α promoter (catalog no. CS204350; Millipore). Primer specificity was confirmed by a single-peak melt curve. Each parameter was assayed in triplicate for three independent experiments.

Flow cytometry and cell viability analysis

GFP$^+$ and GFP$^-$ HeLa cells transiently expressing pCMV-miR-30c-2–GFP or empty vector control were sorted using a cell sorter (FACSAria III; BD) for gene expression analysis. For cell viability assays, cells expressing either the pEZX-AM02-anti–miR-30c-2*–mCherry or the pEZX-AM02-inhibitor control-mCherry vector were trypsinized, pelleted, washed with PBS, and then resuspended and incubated for 15 min in 100 µl of staining cocktail (85 µl PBS, 10 µl Annexin V buffer [BD], and 5 µl 7-AAD [BD]). Cells were then pelleted, aspirated to remove staining cocktail, and resuspended in 1 ml PBS for flow cytometry analysis. For each sample, 100,000 events were collected based on forward and side scatter characteristics. Discriminating gates were set to assess 7-AAD fluorescence in cells positive for mCherry.

Statistical analysis

Statistical differences between groups were assessed using the Student's t test. A 95% confidence interval was considered statistically significant. For each dataset, $n \geq 3$ and $P < 0.05$; error bars represent means ± SD.

Online supplemental material

Fig. S1 depicts analysis of *DNAJB9* and *DDIT3* expression in Tm-treated HeLa cells overexpressing miR-30c-2*. Fig. S2 reports the kinetics of induction of miR-30c-2* and *Xbp1* in Tm-treated NIH-3T3 cells. Fig. S3 depicts analysis of *DNAJB9*, *SRP54A*, *EDEM1*, and *DDIT3* expression in Tm-treated HeLa cells overexpressing anti–miR-30c-2*. Online supplemental material is available at http://www.jcb.org/cgi/content/full/jcb.201201077/DC1.

References

Adachi, Y., K. Yamamoto, T. Okada, H. Yoshida, A. Harada, and K. Mori. 2008. ATF6 is a transcription factor specializing in the regulation of quality control proteins in the endoplasmic reticulum. *Cell Struct. Funct.* 33:75–89. http://dx.doi.org/10.1247/csf.07044

Ambros, V., B. Bartel, D.P. Bartel, C.B. Burge, J.C. Carrington, X. Chen, G. Dreyfuss, S.R. Eddy, S. Griffiths-Jones, M. Marshall, et al. 2003. A uniform system for microRNA annotation. *RNA*. 9:277–279. http://dx.doi.org/10.1261/rna.2183803

Baeuerle, P.A., and D. Baltimore. 1988. I kappa B: a specific inhibitor of the NF-kappa B transcription factor. *Science*. 242:540–546. http://dx.doi.org/10.1126/science.3140380

Bartel, D.P. 2009. MicroRNAs: target recognition and regulatory functions. *Cell*. 136:215–233. http://dx.doi.org/10.1016/j.cell.2009.01.002

Bartoszewski, R., J.W. Brewer, A. Rab, D.K. Crossman, S. Bartoszewska, N. Kapoor, C. Fuller, J.F. Collawn, and Z. Bebok. 2011. The unfolded protein response (UPR)-activated transcription factor X-box-binding protein 1 (XBP1) induces micro-RNA-346 expression that targets the human antigen peptide transporter 1 (TAP1) mRNA and governs immune regulatory genes. *J. Biol. Chem.* 286:41862–41870. http://dx.doi.org/10.1074/jbc.M111.304956

Behrman, S., D. Acosta-Alvear, and P. Walter. 2011. A CHOP-regulated microRNA controls rhodopsin expression. *J. Cell Biol.* 192:919–927. http://dx.doi.org/10.1083/jcb.201010055

Bommiasamy, H., S.H. Back, P. Fagone, K. Lee, S. Meshinchi, E. Vink, R. Sriburi, M. Frank, S. Jackowski, R.J. Kaufman, and J.W. Brewer. 2009. ATF6alpha induces XBP1-independent expansion of the endoplasmic reticulum. *J. Cell Sci.* 122:1626–1636. http://dx.doi.org/10.1242/jcs.045625

Brockman, J.A., D.C. Scherer, T.A. McKinsey, S.M. Hall, X. Qi, W.Y. Lee, and D.W. Ballard. 1995. Coupling of a signal response domain in I kappa B alpha to multiple pathways for NF-kappa B activation. *Mol. Cell. Biol.* 15:2809–2818.

Calfon, M., H. Zeng, F. Urano, J.H. Till, S.R. Hubbard, H.P. Harding, S.G. Clark, and D. Ron. 2002. IRE1 couples endoplasmic reticulum load to secretory capacity by processing the XBP-1 mRNA. *Nature*. 415:92–96. http://dx.doi.org/10.1038/415092a

Chen, H., and L. Qi. 2010. SUMO modification regulates the transcriptional activity of XBP1. *Biochem. J.* 429:95–102. http://dx.doi.org/10.1042/BJ20100193

Deng, J., P.D. Lu, Y. Zhang, D. Scheuner, R.J. Kaufman, N. Sonenberg, H.P. Harding, and D. Ron. 2004. Translational repression mediates activation of nuclear factor kappa B by phosphorylated translation initiation factor 2. *Mol. Cell. Biol.* 24:10161–10168. http://dx.doi.org/10.1128/MCB.24.23.10161-10168.2004

Frank, F., N. Sonenberg, and B. Nagar. 2010. Structural basis for 5′-nucleotide base-specific recognition of guide RNA by human AGO2. *Nature*. 465:818–822. http://dx.doi.org/10.1038/nature09039

Harding, H.P., I. Novoa, Y. Zhang, H. Zeng, R. Wek, M. Schapira, and D. Ron. 2000a. Regulated translation initiation controls stress-induced gene expression in mammalian cells. *Mol. Cell*. 6:1099–1108. http://dx.doi.org/10.1016/S1097-2765(00)00108-8

Harding, H.P., Y. Zhang, A. Bertolotti, H. Zeng, and D. Ron. 2000b. Perk is essential for translational regulation and cell survival during the unfolded protein response. *Mol. Cell*. 5:897–904. http://dx.doi.org/10.1016/S1097-2765(00)80330-5

Harding, H.P., Y. Zhang, H. Zeng, I. Novoa, P.D. Lu, M. Calfon, N. Sadri, C. Yun, B. Popko, R. Paules, et al. 2003. An integrated stress response regulates amino acid metabolism and resistance to oxidative stress. *Mol. Cell*. 11:619–633. http://dx.doi.org/10.1016/S1097-2765(03)00105-9

Haze, K., H. Yoshida, H. Yanagi, T. Yura, and K. Mori. 1999. Mammalian transcription factor ATF6 is synthesized as a transmembrane protein and activated by proteolysis in response to endoplasmic reticulum stress. *Mol. Biol. Cell*. 10:3787–3799.

Hu, P., Z. Han, A.D. Couvillon, R.J. Kaufman, and J.H. Exton. 2006. Autocrine tumor necrosis factor alpha links endoplasmic reticulum stress to the membrane death receptor pathway through IRE1alpha-mediated NF-kappaB activation and down-regulation of TRAF2 expression. *Mol. Cell. Biol.* 26:3071–3084. http://dx.doi.org/10.1128/MCB.26.8.3071-3084.2006

Huntzinger, E., and E. Izaurralde. 2011. Gene silencing by microRNAs: contributions of translational repression and mRNA decay. *Nat. Rev. Genet.* 12:99–110. http://dx.doi.org/10.1038/nrg2936

Iwakoshi, N.N., A.H. Lee, P. Vallabhajosyula, K.L. Otipoby, K. Rajewsky, and L.H. Glimcher. 2003. Plasma cell differentiation and the unfolded protein response intersect at the transcription factor XBP-1. *Nat. Immunol.* 4:321–329. http://dx.doi.org/10.1038/ni907

Jiang, H.Y., S.A. Wek, B.C. McGrath, D. Scheuner, R.J. Kaufman, D.R. Cavener, and R.C. Wek. 2003. Phosphorylation of the alpha subunit of eukaryotic initiation factor 2 is required for activation of NF-kappaB in response to diverse cellular stresses. *Mol. Cell. Biol.* 23:5651–5663. http://dx.doi.org/10.1128/MCB.23.16.5651-5663.2003

Kaneko, M., Y. Niinuma, and Y. Nomura. 2003. Activation signal of nuclear factor-kappa B in response to endoplasmic reticulum stress is transduced via IRE1 and tumor necrosis factor receptor-associated factor 2. *Biol. Pharm. Bull.* 26:931–935. http://dx.doi.org/10.1248/bpb.26.931

Karin, M., Y. Cao, F.R. Greten, and Z.-W. Li. 2002. NF-kappaB in cancer: from innocent bystander to major culprit. *Nat. Rev. Cancer.* 2:301–310. http://dx.doi.org/10.1038/nrc780

Kawai, T., and S. Akira. 2010. The role of pattern-recognition receptors in innate immunity: update on Toll-like receptors. *Nat. Immunol.* 11:373–384. http://dx.doi.org/10.1038/ni.1863

Krek, A., D. Grün, M.N. Poy, R. Wolf, L. Rosenberg, E.J. Epstein, P. MacMenamin, I. da Piedade, K.C. Gunsalus, M. Stoffel, and N. Rajewsky. 2005. Combinatorial microRNA target predictions. *Nat. Genet.* 37:495–500. http://dx.doi.org/10.1038/ng1536

Lai, E.C. 2002. Micro RNAs are complementary to 3′ UTR sequence motifs that mediate negative post-transcriptional regulation. *Nat. Genet.* 30:363–364. http://dx.doi.org/10.1038/ng865

Lee, A.H., N.N. Iwakoshi, and L.H. Glimcher. 2003. XBP-1 regulates a subset of endoplasmic reticulum resident chaperone genes in the unfolded protein response. *Mol. Cell. Biol.* 23:7448–7459. http://dx.doi.org/10.1128/MCB.23.21.7448-7459.2003

Lee, J., C. Sun, Y. Zhou, J. Lee, D. Gokalp, H. Herrema, S.W. Park, R.J. Davis, and U. Ozcan. 2011. p38 MAPK-mediated regulation of Xbp1s is crucial for glucose homeostasis. *Nat. Med.* 17:1251–1260. http://dx.doi.org/10.1038/nm.2449

Leung, A.K.L., and P.A. Sharp. 2010. MicroRNA functions in stress responses. *Mol. Cell.* 40:205–215. http://dx.doi.org/10.1016/j.molcel.2010.09.027

Lewis, B.P., C.B. Burge, and D.P. Bartel. 2005. Conserved seed pairing, often flanked by adenosines, indicates that thousands of human genes are microRNA targets. *Cell.* 120:15–20. http://dx.doi.org/10.1016/j.cell.2004.12.035

Li, Q., and I.M. Verma. 2002. NF-kappaB regulation in the immune system. *Nat. Rev. Immunol.* 2:725–734. http://dx.doi.org/10.1038/nri910

Majumder, M., C. Huang, M.D. Snider, A.A. Komar, J. Tanaka, R.J. Kaufman, D. Krokowski, and M. Hatzoglou. 2012. A novel feedback loop regulates the response to endoplasmic reticulum stress via the cooperation of cytoplasmic splicing and mRNA translation. *Mol. Cell. Biol.* 32:992–1003. http://dx.doi.org/10.1128/MCB.06665-11

Martinon, F., X. Chen, A.-H.L. Lee, and L.H. Glimcher. 2010. TLR activation of the transcription factor XBP1 regulates innate immune responses in macrophages. *Nat. Immunol.* 11:411–418. http://dx.doi.org/10.1038/ni.1857

Okamura, K., M.D. Phillips, D.M. Tyler, H. Duan, Y.T. Chou, and E.C. Lai. 2008. The regulatory activity of microRNA* species has substantial influence on microRNA and 3′ UTR evolution. *Nat. Struct. Mol. Biol.* 15:354–363. http://dx.doi.org/10.1038/nsmb.1409

Ro, S., C. Park, D. Young, K.M. Sanders, and W. Yan. 2007. Tissue-dependent paired expression of miRNAs. *Nucleic Acids Res.* 35:5944–5953. http://dx.doi.org/10.1093/nar/gkm641

Romero-Ramirez, L., H. Cao, D. Nelson, E. Hammond, A.-H. Lee, H. Yoshida, K. Mori, L.H. Glimcher, N.C. Denko, A.J. Giaccia, et al. 2004. XBP1 is essential for survival under hypoxic conditions and is required for tumor growth. *Cancer Res.* 64:5943–5947. http://dx.doi.org/10.1158/0008-5472.CAN-04-1606

Ron, D., and P. Walter. 2007. Signal integration in the endoplasmic reticulum unfolded protein response. *Nat. Rev. Mol. Cell Biol.* 8:519–529. http://dx.doi.org/10.1038/nrm2199

Shaffer, A.L., M. Shapiro-Shelef, N.N. Iwakoshi, A.H. Lee, S.B. Qian, H. Zhao, X. Yu, L. Yang, B.K. Tan, A. Rosenwald, et al. 2004. XBP1, downstream of Blimp-1, expands the secretory apparatus and other organelles, and increases protein synthesis in plasma cell differentiation. *Immunity.* 21:81–93. http://dx.doi.org/10.1016/j.immuni.2004.06.010

Shakhov, A.N., M.A. Collart, P. Vassalli, S.A. Nedospasov, and C.V. Jongeneel. 1990. κB-type enhancers are involved in lipopolysaccharide-mediated transcriptional activation of the tumor necrosis factor α gene in primary macrophages. *J. Exp. Med.* 171:35–47. http://dx.doi.org/10.1084/jem.171.1.35

Shen, X., R.E. Ellis, K. Lee, C.Y. Liu, K. Yang, A. Solomon, H. Yoshida, R. Morimoto, D.M. Kurnit, K. Mori, and R.J. Kaufman. 2001. Complementary signaling pathways regulate the unfolded protein response and are required for *C. elegans* development. *Cell.* 107:893–903. http://dx.doi.org/10.1016/S0092-8674(01)00612-2

Tabas, I., and D. Ron. 2011. Integrating the mechanisms of apoptosis induced by endoplasmic reticulum stress. *Nat. Cell Biol.* 13:184–190. http://dx.doi.org/10.1038/ncb0311-184

Wang, F.-M., Y.-J. Chen, and H.-J. Ouyang. 2011. Regulation of unfolded protein response modulator XBP1s by acetylation and deacetylation. *Biochem. J.* 433:245–252. http://dx.doi.org/10.1042/BJ20101293

Wu, J., D.T. Rutkowski, M. Dubois, J. Swathirajan, T. Saunders, J. Wang, B. Song, G.D. Yau, and R.J. Kaufman. 2007. ATF6alpha optimizes long-term endoplasmic reticulum function to protect cells from chronic stress. *Dev. Cell.* 13:351–364. http://dx.doi.org/10.1016/j.devcel.2007.07.005

Yamamoto, K., T. Sato, T. Matsui, M. Sato, T. Okada, H. Yoshida, A. Harada, and K. Mori. 2007. Transcriptional induction of mammalian ER quality control proteins is mediated by single or combined action of ATF6alpha and XBP1. *Dev. Cell.* 13:365–376. http://dx.doi.org/10.1016/j.devcel.2007.07.018

Yanagitani, K., Y. Kimata, H. Kadokura, and K. Kohno. 2011. Translational pausing ensures membrane targeting and cytoplasmic splicing of XBP1u mRNA. *Science.* 331:586–589. http://dx.doi.org/10.1126/science.1197142

Yang, J.-S., M.D. Phillips, D. Betel, P. Mu, A. Ventura, A.C. Siepel, K.C. Chen, and E.C. Lai. 2011. Widespread regulatory activity of vertebrate microRNA* species. *RNA.* 17:312–326. http://dx.doi.org/10.1261/rna.2537911

Ye, J., R.B. Rawson, R. Komuro, X. Chen, U.P. Davé, R. Prywes, M.S. Brown, and J.L. Goldstein. 2000. ER stress induces cleavage of membrane-bound ATF6 by the same proteases that process SREBPs. *Mol. Cell.* 6:1355–1364. http://dx.doi.org/10.1016/S1097-2765(00)00133-7

Yoshida, H., T. Matsui, A. Yamamoto, T. Okada, and K. Mori. 2001. XBP1 mRNA is induced by ATF6 and spliced by IRE1 in response to ER stress to produce a highly active transcription factor. *Cell.* 107:881–891. http://dx.doi.org/10.1016/S0092-8674(01)00611-0